RSC Advances

1 **Production of Phenolics via Photocatalysis of Ball Milled Lignin-TiO$_2$**

2 **Mixtures in Aqueous Suspension**

3 **Vaishakh Nair,[a] Piyali Dhar,[a] R.Vinu [a,b,*]**

4 [a] Department of Chemical Engineering, Indian Institute of Technology Madras, Chennai –

5 600036, India

6 [b] National Center for Combustion Research and Development, Indian Institute of Technology

7 Madras, Chennai – 600036, India

8

9

10

11

12

13

14

15

16

17

18

19

20

21

[*] Corresponding Author. Phone: +91-44-2257 4187. E-mail: vinu@iitm.ac.in (R. Vinu)

Abstract

In this study, photocatalytic conversion of lignin to valuable phenolic and aromatic compounds is demonstrated by subjecting ball milled mixtures of lignin and TiO_2 to ultraviolet (UV) radiation. Unlike a majority of the existing studies that reported photocatalytic degradation of lignin that is solubilized in alkaline medium, this study evaluates the decomposition of lignin under natural conditions in aqueous medium. In order to facilitate better contact between lignin and nano-TiO_2, the two materials were ball milled in presence of different media, viz. no solvent, hexane, acetone and water. The ball milled mixtures were characterized using powder XRD, FT-IR and photoluminescence spectroscopy, and scanning electron microscopy. Intimate contact between lignin and TiO_2 was achieved using water and acetone as solvents in wet milling. Photocatalysis experiments were conducted in a batch photoreactor. The aqueous phase products were analyzed using UV-visible spectroscopy, MALDI-TOF and GC mass spectrometry, while the molecular weight of solid lignin was analyzed using GPC. Ball milling resulted in the formation of phenolic compounds even during dark mixing of the mixtures prior to photocatalysis. Ball milled mixtures obtained using acetone and water resulted in high yield of phenolic compounds after 3-4 hours of UV exposure. At long UV exposure periods, the phenolics production got saturated, possibly due to the deactivation of TiO_2 active sites by the intermediates. The main organic compounds produced during photocatalysis include ethyl benzene, acetovanillone, syringaldehyde, acetosyringone, vanillin, 2,6-dimethoxy benzoquinone and diisobutyl phthalate. Free radical depolymerization reactions of lignin mediated by active hydroxyl and superoxide radicals are responsible for the observed products.

Keywords: Lignin; photocatalysis; TiO_2; ball milling; phenols; characterization

RSC Advances

1. Introduction

Current research in the fields of energy generation and environmental conservation is focused on utilizing lignocellulosic biomass for obtaining valuable chemicals, materials and fuels. It is believed that the increase in dependence on renewables-based economy would help in preserving the depleting fossil fuel-based industries.[1,2] Cellulose, hemicellulose and lignin are the major components of lignocellulosic biomass. Lignin, which constitutes 10–25 wt.% of lignocellulosic biomass, is the second most abundant natural polymer.[3] Cellulosic ethanol bio-refineries and paper industries utilize cellulose and hemicellulose, and reject lignin as the major byproduct. The waste lignin is primarily utilized for power generation via combustion, which is a high volume, yet low value application. Importantly, not more than 2% of the total 70 million tons of lignin produced is used in the production of phenolic resins, polyurethane foams and bio-dispersants.[3,4] Lignin is the only naturally synthesized aromatic biopolymer made up of three phenyl propane units like *p*-coumaryl alcohol, coniferyl alcohol, and sinapyl alcohol. These monomers are connected by ether and carbon-carbon bonds such as β-aryl ether (β-O-4), α-aryl ether (α-O-4), diphenyl ether (4-O-5) and biphenyl (5–5).[3,5] Therefore, it can be regarded as a rich source of phenols, aromatic and aliphatic compounds. However, it is difficult to deconstruct lignin to various value added products because of its complex crosslinked structure.

The major lignin depolymerization techniques include biochemical, catalytic oxidation, thermochemical, electrooxidation, ionic liquid treatment and photooxidation methods.[1,3,5-9] Thermochemical conversion of lignin via catalytic fast pyrolysis is a well-studied process that yields simple phenols, guaiacols and syringols as the key products.[5,10] Nevertheless, lignin tars contain a complex mixture of lignin oligomers, which are not easily recoverable. Photocatalysis is an advanced oxidation process that involves the generation of highly reactive hydroxyl

67   radicals, which mediate a number of organic oxidation reactions.[11] TiO_2 is a promising

68   photocatalyst and has particular potential for lignin degradation. Owing to its non-toxic nature,

69   physicochemical stability and strong oxidizing potential, TiO_2 is a photocatalyst of choice for a

70   wide variety of reactions including destruction of organic pollutants like dyes, phenolics, volatile

71   organics, pesticides and pharmaceutical compounds.[12,13]

72   The presence of di- and tri-substituted benzene conjugated to aromatic carbonyl, α,β-

73   unsaturated carbonyl, quinone and catechol moieties in lignin lead to ultraviolet (UV) and visible

74   light absorption.[14] As a result, lignin can be effectively depolymerized via photooxidation in

75   presence of oxygen. Earlier studies on delignification of unbleached kraft pulps from paper

76   industry using UV light demonstrated c.a. 85% removal of lignin, which was measured by the

77   kappa number.[14] The presence of oxygen and acidic or alkaline medium were found to be

78   detrimental in the removal of lignin. Contrastingly, irradiation under inert N_2 atmosphere led to

79   condensation of lignin ring fragments, and hence, an effective increase in molecular weight.

80   Studies that utilized lignin model compounds along with singlet oxygen quenching molecules

81   unraveled the mechanism of photooxidation, which involves the cleavage of β-O-4 aryl ether

82   bond and hydrogen abstraction reactions to form hydroperoxides, phenol, guaiacol,

83   acetoveratrone, stilbene, syringol, vanillin, phenyl coumarone, dibenzodioxocin and their

84   derivatives.[14,15] Very few studies are available on heterogeneous photocatalytic decomposition of

85   lignin, and a summary of the existing studies and their salient features are listed in Table 1.[9,16-23]

86   Importantly, as lignin is insoluble in aqueous medium in the absence of externally added alkali,

87   the existing studies were performed at basic pH. From the mass spectrum of lignin dissolved in

88   alkaline medium shown in Figure S1 (in Supplementary Data), it is evident that a number of low

89   molecular weight fragments (<300 Da) are produced via lignin depolymerization reactions

90   induced by the high concentration of NaOH. Therefore, photocatalysis of this mixture results in

91   the degradation of these small molecules more than the degradation of the polymeric structure of

92   lignin itself. On an application viewpoint, this also results in the usage of large quantities of

93   alkali for the dissolution of lignin. Furthermore, the mechanism of lignin/lignin oligomer

94   decomposition will be significantly influenced by the presence of alkali. This work is an attempt

95   to understand the mechanism of photocatalytic decomposition of lignin in the absence of

96   externally added reagents. To the best of our knowledge, this work is the first of its kind in the

97   following aspects: (i) utilization of lignin in solid form in aqueous medium in photocatalysis

98   experiments, and (ii) pretreatment of lignin along with the photocatalyst, viz. nano-TiO_2, via ball

99   milling to induce better contact between lignin and TiO_2.

100   Pretreatment of lignin is essential for improving the yield of phenolic compounds in any

101   conversion process. Many physical and chemical pretreatment methods like ball milling, dilute

102   acid, steam, hot water, ionic liquid and organic solvent treatments have been successfully

103   employed to overcome the recalcitrance of biomass and lignin, and improve the extraction of

104   products.[24] Among these pretreatment techniques, ball milling is a promising pretreatment

105   process in terms of polydispersity reduction and reactivity improvement. Yamashita et al.[25]

106   revealed that a combination of ball milling and phosphoric acid is an effective pretreatment

107   method for the production of ethanol from paper sludge. In addition, other investigations

108   indicated that wet ball milling (WM) is better than dry ball milling (DM).[26] The use of planetary

109   mill-based pretreatment is an efficient and environmentally-friendly method as it imparts

110   artificial gravity to the grinding medium via a centrifugal force field. This causes a non-uniform

111   field of centripetal acceleration. As a result, the balls in planetary mill have notably higher

112   impact energies.[27] Importantly, milling is shown to produce relatively lesser amount of soluble

113   phenolics compared to alkali treatment.[27]

114   The objectives of this work are four fold: (i) preparation of lignin-TiO_2 mixtures in a ball

115   mill via dry milling and wet milling (using different solvents like water, hexane and acetone), (ii)

116   characterization of the mixtures using various techniques such as Fourier transform infrared

117   spectroscopy, photoluminescence spectroscopy, powder X-ray diffraction, and scanning electron

118   microscopy, (iii) photo degradation of aqueous lignin-TiO_2 suspensions and evaluation of

119   concentration of total phenolics by UV-visible spectrophotometer, and (iv) identification of

120   various phenolic compounds using mass spectrometry and molecular weight of solid phase lignin

121   by gel permeation chromatography.

122   **2. Experimental Section**

123   **2.1. Materials**

124   Commercial lignin was procured from Asian Lignin Manufacturing (ALM), India. This

125   lignin is extracted from non-woody biomasses like wheat straw and sarkanda grass by soda

126   pulping process using aq. NaOH.[28] The number average and weight average molecular weights

127   of ALM lignin are reported to be 1000 Da and 2500-3400 Da, respectively.[28] Commercial TiO_2

128   (Aeroxide® P25) was obtained from Sigma Aldrich. Water, n-hexane (Merck) and acetone

129   (Sisco Research Laboratories Pvt. Ltd. India) were used as solvents in the wet ball milling

130   process. Double deionized water was used as the reaction medium for photocatalysis

131   experiments. The solvents, dichloromethane, tetrahydrofuran (THF), and dimethyl formamide

132   (DMF), were procured from Merck, India. o-Nitrobenzaldehyde (Avra Synthesis Pvt. Ltd., India)

133   was used to determine the intensity of the ultraviolet (UV) lamp via actinometry.[29]

2.2. Preparation of Lignin-TiO$_2$ Mixtures

Lignin and TiO$_2$ were thoroughly mixed in a planetary ball mill (Fritsch Pulverisette) equipped with zirconia milling jar of 250 mL capacity. The jar containing 100 steel balls of 10 mm diameter was loaded with 5 g of lignin-TiO$_2$ mixture (1:1 w/w), and milled at 120 rpm for 6 hours. The sample thus obtained is called as dry milled mixture (DM). For wet milling, solvents such as water, hexane or acetone were also added to the lignin-TiO$_2$ mixture at 1:2 w/w of mixture:solvent ratio before the grinding process. The choice of these solvents is based on their widely different polarities (water-highly polar, acetone-medium polar, hexane-non-polar). The mixtures obtained after wet milling are henceforth denoted as WMW, WMH and WMA, corresponding to water, hexane and acetone, respectively. The mixtures thus obtained were filtered and dried at 40 $^{\circ}$C. The dried mixtures were washed with water and then vacuum filtered. The residue was dried in hot air oven at 100 $^{\circ}$C overnight. The recovery of the solids was calculated as the ratio of final dried mass of ball milled samples to the initial mass of lignin-TiO$_2$ mixture. Lignin, without TiO$_2$, was also ball milled in the presence and absence of the above solvents in order to perform control experiments.

2.3. Characterization of Lignin-TiO$_2$ Mixtures

Powder X-ray diffractograms (XRD) of lignin, TiO$_2$ and the ball milled mixtures were collected in D8 Discover (Bruker) diffractometer using Cu-K$_\alpha$ radiation. Fourier transform infrared (FT-IR) spectra were obtained in an Agilent Cary 660 FT-IR spectrometer in the wavenumber range of 400–4000 cm^{-1} in transmittance mode at a resolution of 2 cm^{-1}. The fine powders were cast in the form of pellets using KBr. The surface morphology and energy dispersive X-ray analyses (EDS) of the mixtures were performed using a Hitachi S-4800 high

156   resolution scanning electron microscope (SEM). The UV absorption spectra of the mixtures were

157   collected in a UV-visible photodiode array (PDA) spectrophotometer (Agilent Cary 8454) by

158   suspending the mixtures in water. Photoluminescence emission (PL) spectra of TiO_2, WMW,

159   WMA, WMH and DM mixtures were recorded in an Agilent Cary Eclipse fluorescence

160   spectrometer at an excitation wavelength of 257 nm. 70 mg of the samples were dry pressed and

161   analyzed to compare the intensities of the samples. Thermogravimetric analyses (TGA) of the

162   mixtures were performed in a SDT Q600 TG analyzer (T.A. Instruments) at 10 ^{o}C min^{-1} under

163   continuous flow of N_2 gas at 100 mL min^{-1}. Typically, 5±0.3 mg of the samples were pyrolyzed

164   and mass loss of the sample with temperature was monitored. Differential mass loss and onset

165   degradation temperature were evaluated.

2.4. Photocatalytic Treatment of Lignin−TiO$_2$ Mixtures

167   Photocatalytic degradation of only lignin, physical mixtures of both untreated and ball

168   milled lignin and TiO_2, and the various mixtures, viz. DM, WMW, WMH and WMA, were

169   carried out in aqueous medium in an annular type photoreactor. It is important to note that the

170   lignin-TiO_2 mixtures were well suspended in water without the dissolution of lignin in alkaline

171   medium. The photoreactor consisted of a jacketed quartz tube containing a high pressure

172   mercury lamp (Philips 125 W) that emits UV radiation at a wavelength of 365 nm. The intensity

173   and photon flux of the UV lamp measured by o-nitrobenzaldehyde actinometry were 1.11×10^{-7}

174   Einstein L^{-1} s^{-1} and 4.82 W m^{-2}, respectively. The temperature of the reaction mixture was

175   maintained at 25±3°C by circulating chilled water through the jacket of the quartz tube. The

176   quartz tube was immersed in the reaction vessel for uniform illumination of the reaction mixture.

177   The details of the photocatalytic reactor can be found elsewhere.[30] Unless otherwise specified,

178   the concentration of lignin-TiO_2 mixture taken for experiments was 2 g L^{-1} in aqueous medium.

179   Prior to illumination, the mixtures were stirred well in the dark to ensure that low molecular

180   weight fragments such as monomers and dimers of lignin are dissolved in the aqueous medium.

181   Typically, dark mixing was carried out until the concentration of phenolics in the aqueous

182   medium reached a constant value. After this period, UV lamp was turned on, and the samples

183   were collected at regular time intervals. The total reaction time was 360 min. Prior to analyses,

184   the aliquots were centrifuged to separate the unreacted solids.

185   **2.5. Characterization of Aqueous Phase Products**

186   The concentration of total phenolics produced was determined using UV-visible PDA

187   spectrophotometer (Agilent Cary 8454). A characteristic peak at 280 nm signified the phenolic

188   compounds. Absorbance vs concentration calibration graph was constructed to quantify the total

189   phenolic compounds using Beer-Lambert's law. For the calibration of total phenolics, lignin was

190   dissolved in alkaline medium. The experiments were repeated three times and the uncertainty in

191   the concentration of total phenolics was within 7%.

192   In order to identify the molecular weight of the compounds produced, the aqueous

193   samples were subjected to Matrix Assisted Laser Desorption-Ionization Time-of-Flight Mass

194   Spectrometry (MALDI-TOF). MALDI-TOF analyses were carried out in a Voyager-DE STR

195   Biospectrometry Workstation (Applied Biosystems). 2,5-Dihydroxybenzoic acid (DHB) was

196   used as the matrix, and the analyses were carried out in negative mode. In order to exactly

197   identify the structure of the compounds, gas chromatography-mass spectrometric (GC/MS)

198   technique was adopted. The lignin degradation products in aqueous medium were extracted in

199   dichloromethane (DCM) solvent, and the DCM extract was injected in Shimadzu QP2010 Plus

200   GC/MS equipped with a capillary column RTi-5 MS column (30 m × 0.25 mm; 0.25 μm film

201 thickness, Restek, USA) .Ultra high pure helium gas (5.5 grade) was used as the carrier gas at a

202 total flow rate of 12.5 mL min^{-1}. 1 μL of the sample was injected at a split ratio of 5:1. The

203 column oven was initially held at 40 ^{o}C for 4 min, followed by heating at a rate of 5 ^{o}C min^{-1} to

204 280 ^{o}C, and finally held at 280 ^{o}C for 10 min. The injector, interface and ion source temperatures

205 were 250 ^{o}C, 280 ^{o}C, and 250 ^{o}C, respectively. The mass spectra of the products were acquired

206 in the m/z range of 40-400 Da. The mass spectra of the unknown peaks were compared with

207 NIST mass spectral database to identify the organic compounds. A minimum cut-off of 85% was

208 set as the search criteria in the NIST database. The salient products were reconfirmed by

209 matching the retention time using pure standards, and quantified by constructing calibration

210 graphs.

2.6. Characterization of Solid Phase Lignin

212 The molecular weight of the degraded lignin in the solid phase was determined using a

213 gel permeation chromatograph (GPC) (Agilent GPC 1260 Infinity series). Lignin was dissolved

214 in DMF-0.1% LiBr solution at a concentration of 3 g L^{-1}. The GPC system consisted of a PLgel

215 5μm MiniMIX-C column (250 mm length × 4.6 mm i.d.), Rheodyne injector, 50 μL sample loop

216 and Agilent differential refractive index detector. THF was used as the mobile phase at 0.3 mL

217 min^{-1}. The column was calibrated using twelve poly(methyl methacrylate) (PMMA) standards

218 ranging in molecular weight from 550 to 2,136,000 g mol^{-1}. The calibration curve was fitted to a

219 5th order polynomial with a regression coefficient of 0.99. The calibration plot and equation are

220 available in Figure S2 (in Supplementary Data).

3. Results and Discussions

3.1. Effect of Ball Milling on Lignin-TiO$_2$ Mixture

10

223   The recovery of solids after ball milling of various lignin-TiO_2 mixtures were 94%, 93%,

224   90% and 70% for DM, WMH, WMW and WMA samples, respectively. Qu et al.[31] reported 95%

225   solid recovery after wet milling lignin with water, which is comparable with our study. The

226   higher weight loss in the case of WMA can be related to the higher solubility of lignin in

227   acetone, which was also observed during the preparation. From Figure 1, visual changes in the

228   appearance of wet milled mixtures using polar solvents like acetone and water are evident. The

229   change in the appearance of WMW and WMA mixtures prepared using polar solvents can be

230   related to the intermolecular interactions of the solvent with lignin and TiO_2.[32-34] The hydroxyl

231   groups of the phenolic molecules present in lignin are likely to form hydrogen bonds with water

232   and acetone.[32] It is found that acetone and water have a strong tendency to fill the oxygen vacant

233   sites in TiO_2.[33] Moreover, these two solvents are reported to alter the bond length of α-O-4

234   linkage, and decrease the electronic levels, viz. HOMO (highest occupied molecular orbital) and

235   LUMO (lowest unoccupied molecular orbital), and band gap of lignin.[35] The interactions are

236   further validated by analyzing the FT-IR and photoluminescence spectra of the mixtures as

237   discussed in the next section.

3.2. Characterization of Different Lignin-TiO_2 Mixtures

239   Figure 2 depicts the XRD patterns of pure TiO_2, lignin and different lignin-TiO_2

240   mixtures. All the lignin-TiO_2 mixtures exhibited peaks at 2θ = 25.3, 37.9, 48.1, 54.3,

241   corresponding to anatase phase of TiO_2 (JCPDS, No. 84-1286), and at 2θ = 27.7, 36.2, 41.4,

242   55.3, corresponding to rutile phase of TiO_2 (JCPDS, No. 88-1175). The XRD pattern of pristine

243   lignin showed no crystalline peaks confirming its amorphous nature. Only for wet milled

244   mixtures with acetone and water, a new peak at 31.7º was visible which is attributed to the

245   incorporation of carbon from lignin onto TiO_2. This is an evidence for strong surface attachment

246   and interactions between TiO_2 and lignin, which is desired. Kim et al.[36] also observed a similar

247   peak in the XRD of TiO_2-carbon composites using rice husk as the carbon precursor at high

248   loading. The crystallite sizes of Aeroxide® TiO_2, DM, WMH, WMA and WMW mixtures were

249   similar, i.e. 28±5 nm.

250   The FT-IR spectra of lignin and different lignin-TiO_2 mixtures (Figure S3 in

251   Supplementary Data) were analyzed to understand the structural modifications in the mixtures

252   caused by any interaction between lignin and TiO_2. The signature peaks of lignin are observed at

253   1720 cm^{-1} (C=O stretch of the carbonyl group mostly attached to β or γ carbon of the propane

254   unit of lignin), 1603 and 1514 cm^{-1} (aromatic C=C stretch of the phenolic groups), 1451, 1425

255   and 1364 cm^{-1} (phenolic O-H bending),[37] and 1326, 1268, 1220, 1121 and 1033 cm^{-1} (condensed

256   guaiacyl and syringyl units of lignin).[31,38] The peak at 1630 cm^{-1} in the FT-IR spectra of TiO_2 is

257   attributed to the bending vibration of co-ordinated H_2O as well as Ti-O-H. The FT-IR spectra of

258   DM and WMH (hexane) lignin-TiO_2 mixtures show the presence of all the above signature peaks

259   of lignin. However, C=O stretching (1720 cm^{-1}) and phenolic O-H bending (1364 cm^{-1})

260   vibrations are not observed with WMW and WMA mixtures. Carbonyl groups (aldehyde and

261   ketone) are not directly associated with aromatic rings of lignin, but are present in α, β, and γ

262   carbons. The absence of carbonyl vibration is an indication that these may be involved in

263   reactions in presence of polar solvents. A marked decrease in wavenumber of aromatic C=C

264   stretching (1603 cm^{-1}) by 10 cm^{-1} was observed for WMA and WMW mixtures. These changes

265   may be due to molecular level interactions between lignin and TiO_2 induced by ball milling in

266   the presence of polar solvents. Parthasarathi et al.[39] showed the existence of hydrogen bonding of

267   type C–H…O, O–H…O in phenol-water clusters via density functional theory calculations,

268   which partly substantiates the shifts in wavenumbers. The phenoxide groups of lignin are known

269   to be neutralized by protonation, which is expected to occur in presence of water.[34] Moreover,

270   acetone and water are known to compete and adsorb onto TiO_2 (100) sites via oxygen (H-"O"-H

271   and H_3C-C(="O")-CH_3).[33] Therefore, two way interactions are envisaged to occur between lignin

272   and polar solvents, and between TiO_2 and polar solvents. These interactions might result in

273   association of lignin with TiO_2 mediated by the solvent molecules.

274   SEM images of lignin and ball milled mixtures are shown in Figure 3. It is observed that

275   the surface of lignin (Figure 3(a)) is non-uniform with micron sized structures. No significant

276   change in surface morphology was observed in the dry milled mixture. However, the particle size

277   and surface morphology of the lignin-TiO_2 mixtures display interesting changes after wet

278   milling. For WMH mixture, the size distribution of lignin-TiO_2 clusters is uniform (Figure 3(b)),

279   while the formation of large sized lignin-TiO_2 aggregates are observed in WMA mixture (Figure

280   3(c)). The morphology of WMW sample in Figure 3(d) showed a smoother surface with

281   distribution of agglomerated particles. Owing to strong hydrophobicity, aggregated islands of

282   lignin molecules could be observed when ball milled with water.[31] The EDS data was analyzed at

283   different spatial locations of the samples to evaluate the percent incorporation of TiO_2 in the

284   surface of lignin (Table S1 in Supplementary Data). It is evident that the incorporation of TiO_2

285   on the surface of the mixtures is 14-18 wt.% of Ti (25-31 wt.% of TiO_2). As EDS technique

286   probes only the sample surface, the rest of TiO_2 (19-25 wt.%) is obviously present within the

287   lignin matrix. Figure S4 (in Supplementary Data) depicts the UV-visible spectra of the lignin-

288   TiO_2 mixtures. A distinct peak at 280 nm for the mixtures signifies the phenolic groups from

289   lignin. The absorption band edges for the various mixtures were 380 nm for WMA, 420 nm for

290   WMW, 436 nm for Aeroxide TiO_2, and 475 for DM. WMH mixture exhibited a very broad band

291   without a specific absorption band edge.

292   Photoluminescence (PL) technique is used to understand the surface processes involving

293   charge carriers, and to evaluate the efficiency of charge carrier trapping, migration and transfer

294   between composite materials.[40,41] Figure 4 depicts the PL emission spectra of TiO_2, dry milled

295   and wet milled lignin-TiO_2 mixtures when excited at 257 nm. The major emission peaks at 410

296   and 483 nm can be attributed to free exciton emission of TiO_2 and Ti^{4+}-OH, respectively.[40] The

297   PL intensity for the ball milled mixtures follows the order: WMH > DM > WMA ≈ WMW.

298   While the reduction in PL intensities of the ball milled lignin-TiO_2 mixtures can be attributed to

299   the low amount of TiO_2 in the samples and sample heterogeneity, these differences can also be

300   attributed to the variation in electron transfer from the excited state of TiO_2 to the new levels or

301   defects introduced by lignin. Importantly, the same trend in PL intensity was observed with

302   samples chosen from different spatial locations of the mixtures. The interactions depend on how

303   well TiO_2 and lignin are mixed. The low intensity or high extent of quenching of fluorescence

304   observed with WMA and WMW mixtures is an indication that the probability of electron transfer

305   to lignin is more, which might lead to a lower recombination of charge carriers. Using quantum

306   chemistry calculations, it is shown that water and acetone greatly modify the electronic states

307   (HOMO and LUMO) and band gap associated with α-O-4 and β-β bonds of lignin.[35] For

308   example, the valence band and conduction band edges of TiO_2 are -7.46 eV (vs vacuum) and -

309   4.26 eV, respectively,[42] and the HOMO and LUMO states of α-O-4 of lignin in water solvent are

310   -5.076 eV and -1.714 eV, respectively.[35] This shows that the electron transfer can occur from

311   conduction band of TiO_2 to HOMO of lignin during excitation. This trapped electron can initiate

312   reactions in lignin. Importantly, the HOMO and LUMO states are said to vary in presence of

313   different solvents. This supports the low PL intensity observed with WMA and WMW mixtures.

314   However, when lignin-TiO_2 mixture is ball milled in the absence of solvent or in presence of a

315   non-polar solvent like hexane, the recombination of charge carriers may be high, and this can

316   lead to a low photocatalytic activity.

317   The thermal stability of the mixtures was evaluated using TGA. Figure 5 depicts the mass

318   loss and differential mass loss profiles of lignin, dry milled and wet milled mixtures of lignin and

319   TiO_2. It is evident that the sample mass remaining at the final temperature, 900 ^{o}C, is

320   significantly more for the mixtures, which is attributed to the presence of TiO_2. The mass loss

321   profiles of WMW and WMA mixtures are less steep in the temperature range of 200-400 ^{o}C,

322   which signifies the slow rate of decomposition. The absence of shoulders at 200 and 250 ^{o}C in

323   the differential mass loss profile was also evident for the WMW mixture. The onset degradation

324   temperature (T_{onset}) follows the trend: WMW (235.5 ^{o}C) > WMA (213 ^{o}C) > lignin (203.2 ^{o}C) >

325   DM, WMH (199.3 ^{o}C). This shows that the WMW and WMA mixtures are more stable than the

326   others, which is indirect evidence that demonstrates the probable interactions between lignin and

327   TiO_2 in mixtures prepared using polar solvents. This also stands as a supporting analysis for the

328   claims made via XRD and PL studies.

329   **3.3. Production of Phenolics During Dark Mixing**

330   Figure 6 depicts the concentration profiles of the phenolic compounds produced during

331   dark mixing and UV illumination under different conditions. It is observed that within 3 h of

332   stirring the lignin-TiO_2 mixtures in the dark, a constant production of phenolics was observed.

333   This is attributed to the dissolution of low molecular weight fragments such as monomers and

334   dimers that are inherently present in the lignin sample or those produced by ball milling. The

335   concentration (in mg L^{-1}) of phenolics produced at the end of 3 h of dark stirring for various

336   mixtures in aqueous medium follows the trend: 268 (WMW) > 133 (WMH) > 124 (DM) > 117

337   (ball milled lignin) > 88 (physical mixture of lignin and TiO_2) $\approx$ 88 (only lignin) > 64 (WMA).

338   With 1 g L^{-1} and 4 g L^{-1} of WMW, 220 and 484 mg L^{-1} of phenolics were produced, respectively,

339   which is expected. A similar trend is also observed when only lignin (in the absence of TiO_2)

340   was ball milled in the absence and presence of different solvents (Figure 7). This shows that ball

341   milling results in the production of more oligomers of lignin that are easily soluble in aqueous

342   medium. The use of acetone as the solvent results in lower production of phenolics during dark

343   mixing. It is important to note that nearly 30% mass loss of lignin was observed when wet milled

344   with acetone. This shows that the use of acetone results in the loss of a majority of the

345   monomeric phenols during the pretreatment step. This means that the dried mixture after

346   pretreatment predominantly contains higher oligomers and long chains of lignin attached to

347   TiO_2. Figure S5 (in Supplementary Data) depicts the particle size distribution of as received

348   lignin and lignin ball milled for 6 h. It is evident that ball milling results in the broadening of

349   lignin particle size distribution towards smaller size range. Moreover, a significant decrease in

350   d_{50} from 22.15 μm (for as received lignin) to 13.4 μm (for ball milled lignin) is also observed.

351   This is also supported by the molecular weight distribution of lignin depicted in Figure S6 (in

352   Supplementary Data). It is evident that this variety of lignin inherently contains a large fraction

353   of low molecular weight fragments in the range of 500-2000 g mol^{-1}, which are easily broken

354   down to phenolics during ball milling process. Depolymerization of lignin is expected to occur

355   during this process by the cleavage of β-aryl ether links.[31] This substantiates the increase in

356   production of phenolics in the initial 3 h period with ball milled lignin compared to untreated

357   lignin. The results also demonstrate that the presence of water during ball milling is favorable as

358   it partially weakens the linkages in lignin, besides aiding in the generation of more surface

359   hydroxyl moieties associated with TiO_2 and lignin.

16

3.4. Production of Phenolics During UV Illumination

360

361   Figure 8 depicts the time evolution of UV-visible spectra during dark mixing and

362   photocatalysis experiments for WMW mixture at 2 g L^{-1} concentration. It is evident that the peak

363   corresponding to total phenolics at 280 nm increases both during dark mixing and UV

364   illumination upto 3 hours. During UV illumination period, no appreciable increase in

365   concentration of phenolic compounds in the aqueous phase could be observed with only lignin or

366   a simple physical mixture of lignin with TiO_2 (Figure 7). This shows that (i) solid lignin does not

367   photodegrade in the absence of any photocatalyst, and (ii) the mere presence of TiO_2 in the

368   suspension along with lignin particles without any intimate contact between the two does not

369   result in the degradation of lignin. The slight decrease in concentration of phenolics in the

370   aqueous phase at long time periods (> 3 h) of UV exposure can be attributed to the degradation

371   of phenolics that were already released during the dark stirring period to the aqueous phase.

372   Photocatalysis of ball milled lignin without TiO_2 also exhibits a flat concentration profile of

373   phenolics in the initial 3 h period of UV illumination, and then shows a drop in concentration.

374   This shows that the presence of TiO_2 in contact with lignin particles is a must for the production

375   of phenolics under UV illumination, and ball milling of lignin without TiO_2 only aids in the

376   production of slightly more amount of phenolics in the dark stirring period.

377   Photocatalysis of DM mixture of lignin and TiO_2 results only in a slight increase in the

378   production of phenolics from 124 to 155 mg L^{-1} in the initial 3 h period, which shows that

379   significant contact between TiO_2 and lignin is not developed by dry milling (Figure 6). However,

380   significant production of phenolics is observed when the wet milled mixtures are subjected to

381   UV irradiation. The increase in phenolics concentration is from 64 to 143 mg L^{-1}, and 133 to 215

382   mg L^{-1} for WMA and WMH mixtures, respectively, at the end of 3 h. Thereafter, the phenolics

17

383   concentration in aqueous phase decreases owing to their photodegradation. Interestingly, the

384   phenolics concentrations are even higher with WMW mixtures. The increase in concentrations

385   are from 220 to 352 mg L^{-1}, 268 to 464 mg L^{-1} and 484 to 623 mg L^{-1} for WMW mixtures of

386   different concentrations, viz. 1 g L^{-1}, 2 g L^{-1} and 4 g L^{-1}, respectively. The percentage

387   contribution by photocatalysis to the overall production of phenolics is also evaluated using the

388   following expression for different lignin-TiO$_2$ mixtures.

389    $$\% \text{ Contribution by photocatalysis} = \frac{C_{max} - C_{(after\ 3\ h\ of\ dark\ mixing)}}{C_{max}} \times 100 \quad\quad (1)$$

390   C_{max} corresponds to the maximum concentration of total phenolics produced, which is usually

391   the concentration from third to fifth hour. Table 2 depicts the values of C_{max} and % contribution

392   by photocatalysis for different mixtures including physical mixtures of ball milled lignin with

393   TiO$_2$ and ball milled lignin+TiO$_2$. It is evident that the addition of TiO$_2$ to ball milled lignin

394   during UV irradiation period (i.e. physical mixture) results in lower production of phenolics in

395   aqueous phase compared to that from ball milled lignin+TiO$_2$ (Figure 7). This substantiates the

396   role played by wet milling in improving the contact between lignin and TiO$_2$, and hence, the

397   electron transfer. Based on the parameter, % contribution by photocatalysis, the mixtures can be

398   ranked as follows: WMA-2 g L^{-1} (55%) > WMW-2 g L^{-1} (42%) > WMH-2 g L^{-1} (38%) ≈ WMW-

399   1 g L^{-1} (38%) > WMW-4 g L^{-1} (22%) ≈ DM-2 g L^{-1} (20%). Even though the maximum

400   concentration of phenolics produced is low with wet milled mixture prepared with acetone, equal

401   contribution from photocatalysis and dark mixing is observed, whereas for high mass

402   concentrations of water based mixtures, more phenolics are formed during dark mixing period

403   compared to photocatalysis. For all the WMW mixtures, the concentration of total phenolics

404   saturated and started to slowly decrease after 4 h of UV illumination. This is also evident from

405   the UV-visible spectra in Figure 8. While this can be ascribed to the mineralization of the

406   aqueous phase phenolics due to the action of UV radiation and TiO_2,[12,30] this also shows the

407   suppression of TiO_2 activity due to the adsorption of lignin oligomers and intermediates on the

408   TiO_2 active sites. It is important to note that when lignin is completely dissolved in the aqueous

409   medium by the use of alkali, the photocatalytic reaction is kinetically controlled, whereas in our

410   experiments, the photocatalytic reaction is both reaction as well as mass transfer controlled.

411   Lignin decomposition occurs exclusively on the catalyst surface mediated by TiO_2. Even though

412   the lignin-TiO_2 solid mixture is continuously stirred during UV illumination, the transfer of

413   phenolic compounds from the solid lignin to aqueous phase is influenced by mass diffusion.

414   It is important to note that the mass ratio of lignin:TiO_2 (1:1 wt./wt.) used in this study is

415   comparable with those employed in existing reports on photocatalytic degradation of lignin (refer

416   Table 1).[9,16,19,21-23] Figure S7 (in Supplementary Data) depicts the concentration profiles of total

417   phenolics produced when 1:1 and 3:1 wt./wt. WMW mixtures of lignin-TiO_2 were subjected to

418   dark stirring and UV irradiation. During the initial dark mixing phase, slightly more phenolics

419   are produced in the aqueous medium from 3:1 lignin-TiO_2 mixture (307 vs 268 mg L^{-1}), which is

420   due to the high amount of lignin in the mixture that depolymerizes to phenolics after the wet

421   milling process. However, during photocatalysis, high concentration of phenolics is produced

422   from equal composition mixture. The % contribution by photocatalysis was only 15% with 3:1

423   lignin-TiO_2, while it was 42% with 1:1 lignin-TiO_2 mixture. This substantiates that equal

424   composition of lignin-TiO_2 is preferred.

425   The reduction in molecular weight of solid phase WMW mixture was probed using GPC.

426   It is evident from Table 3 that ball milling results in a slight drop in M_w of lignin (1980-1777 g

427   mol^{-1}). A similar magnitude of decrease in M_w is also observed during dark stirring period (1777-

428   1590 g mol^{-1}). This shows that the monomers/oligomers that are formed during the ball milling

429   pretreatment are dissolved in aqueous medium. Nevertheless, UV photocatalysis causes a

430   gradual and significant reduction of M_w of lignin (1590-1040 g mol^{-1}). This is also in line with

431   the high production of phenolics in the aqueous phase from WMW mixture during UV

432   irradiation. From the molecular weight distribution graph in Figure S6 (in Supplementary Data),

433   it is evident that the fraction of high molecular weight lignin decreases, while that of low mass

434   fragments (<200 g mol^{-1}) increases with UV treatment. Such a significant change in M_w was not

435   observed with other ball milled mixtures and physical mixtures of lignin and TiO_2. For example,

436   with DM, WMH and WMA mixtures, the decrease in M_w after 6 h of UV treatment was less than

437   400 g mol^{-1}. From the GPC analysis, it can be concluded that although a significant decrease in

438   M_w of lignin is achieved via UV photocatalysis, a significant fraction in the molecular weight

439   range of 800-3000 g mol^{-1} is unconverted.

440   The various reactions taking place during photocatalysis include charge carrier generation

441   (conduction band electrons and valence band holes), generation of active hydroxyl radicals

442   (OH•) via (a) hole pathway involving the reaction of holes with surface OH$^-$ groups and water,

443   and (b) electron pathway involving the reaction of electrons with dissolved oxygen, superoxide

444   radicals, and H_2O_2 in a series of steps. [12,13,43] The generation of highly reactive OH• radicals can

445   result in the degradation of lignin due to the scission of α-O-4 and β-O-4 bonds. This results in

446   the generation of alkoxy, benzyl and alkyl free radicals that take part in a variety of lignin

447   depolymerization reactions to form low molecular weight phenolics and lignin fragments. The

448   OH• radicals can also directly attack the phenyl rings of lignin to form catechol, resorcinol and

449   hydroquinone.[43] Moreover, the H$^+$ ions generated (as a by-product of reaction of holes with

450   water) can also react with conduction band electrons to produce more H•,[11] which take part in

451 hydrogen abstraction reactions. Effectively, the availability of H• for H-abstraction reactions is

452 greatly improved via photocatalysis. As long chain molecules/oligomers of lignin are insoluble

453 in aqueous medium, they are either in contact with TiO_2 or stay in the suspension. The

454 degradation products of lignin, primarily phenolics and dimers, can also block and deactivate the

455 TiO_2 active sites, and lead to the saturation of phenolics production at long time periods. In order

456 to probe the identity of the various products produced during dark mixing and photocatalysis,

457 mass spectrometric characterization of the products was carried out.

3.5. Identification of Products via Mass Spectrometry

459 MALDI-TOF mass spectra of the aqueous phase samples from different experiments are

460 shown in Figure 9. As the reported intensities in the graph are normalized with respect to the

461 DHB peak, the various curves can be compared. It is evident that with DM and WMH mixtures,

462 the production of phenolics in the low mass range is insignificant with very low intensities.

463 However, with WMA and WMH mixtures, higher production of lignin monomers and dimers

464 with molecular weights 168, 184, 196, 206, 233, 249, 288, 315, 320, 327, 340 and 358 g mol^{-1}

465 are observed. Importantly, it can be noticed that a number of peaks are spaced at intervals of c.a.

466 30 mass units, which signifies the difference between a guaiacol and syringol intermediate (that

467 varies by an -OCH_3 group). Lignin monomeric units such as phenyl propane guaiacol (168) and

468 phenyl propane syringol (196) are also observed.[9] Moreover, with increase in photocatalysis

469 time, increase in intensity of the major peaks is also observed for the WMW mixture, which

470 shows the increase in concentration of the phenolic compounds. Figure 10 depicts the GC/MS

471 total ion chromatograms of the DCM extract obtained after 3 h of dark mixing of the WMW

472 mixture, and after 1 h and 3 h of UV treatment. The structure, molecular weight and the typical

473 mass fragments observed for the major phenolic compounds are listed in Table 4. The listed

474   compounds are identified with more than 90% confidence based on NIST mass spectral database.

475   It is evident that styrene, vanillin, acetyl vanillin and acetosyringone are the major products

476   obtained after dark stirring, while a number of other compounds are produced after subjecting

477   the mixture to UV irradiation. For example, dialkyl phthalates are reported to be the major

478   products during lignin depolymerization via hydrogen-free hydrogenolysis in presence of

479   hydrogen donor solvents and metallic catalysts like noble metal-doped Al-SBA-15.[44] The

480   formation of diisobutyl phthalate in aqueous phase photocatalysis shows that mild

481   hydrogenolysis of lignin might occur in the case of WMW mixture. The molecular weight of a

482   number of these compounds also matches with the MALDI-TOF mass spectra in Figure 9.

483   Figure 11 shows the variation of concentration of the major compounds present in DCM

484   extract after different treatment durations. It is interesting to note that styrene concentration

485   drops to zero after the mixture is irradiated, while ethyl benzene production increases drastically.

486   Maximum production of ethyl benzene is observed at 1 h of irradiation. Vanillin and acetyl

487   vanillin production decreases after UV-irradiation, and an increase in production of

488   acetovanillone is observed. Syringaldehyde and acetosyringone production continuously

489   increases with irradiation time. The overall mass conversion of lignin to organic compounds in

490   the total time period including dark stirring and photocatalysis is found to be in the range of 17-

491   20 wt.% for TiO_2-lignin mixtures obtained by wet milling in presence of water. In order to

492   understand the structure of lignin that is used in the experiments, and the similarity of the

493   products obtained via photocatalysis versus fast pyrolysis, which is a reasonably well established

494   technique, analytical pyrolysis of the lignin sample was performed in a micropyrolyzer coupled

495   with GC/MS (Py-GC/MS). Table S2 (in Supplementary Data) depicts the typical products

496   obtained and the relative area% contributions. Based on the products obtained from Py-GC/MS,

497   the contribution of coniferyl, sinapyl and coumaryl units to the total phenolics present in lignin is

498   found to be 56%, 28% and 16%, respectively. This is also in agreement with a literature report.[28]

499   This shows that ALM lignin contains a significant fraction of sinapyl units, which is observed as

500   syringol derivatives after photocatalytic depolymerization. It is evident that the major products

501   formed during photocatalysis, including acetosyringone, acetovanillone, syringaldehyde and

502   vanillin, are also observed in fast pyrolysis. This shows that the mechanism of transformation of

503   lignin and its oligomers to phenolic compounds in both these processes follows a free radical

504   pathway involving the cleavage of alkyl-aryl ether (α-O-4 and β-O-4), aryl-aryl ether (4-O-5)

505   and aryl-aryl (5-5) bonds, hydrogen abstraction and β-scission reactions. While thermal energy is

506   the main driving force for these bond fission reactions in thermolysis, UV radiation and the •OH

507   radicals initiate these reactions in photocatalysis. Importantly, hydroxyl radicals can react with

508   benzene ring via electrophilic addition and cause the cleavage of α-O-4 or β-O-4 ether links in

509   lignin.[15] As a result, OH group substitution is achieved. The formation of dimethoxy

510   benzoquinone was earlier proposed to occur by the action of singlet oxygen ($^1O_2$) or superoxide

511   radicals ($O_2^{•-}$) on the phenolic ring, which results in the cleavage of the bond between aromatic

512   and the α-carbon.[15] Dimethoxy benzoquinone is also formed during ionic liquid assisted

513   depolymerization of lignin. The decrease in concentration of acetyl vanillin on UV irradiation

514   shows that deacetylation reaction also occurs during photocatalysis. Moreover, demethylation,

515   dealkoxylation and hydroxylation are some other reactions mediated by hydroxyl radicals.[15] The

516   first two reactions convert methoxy substituents to hydroxy substituents. Thus, sinapyl

517   derivatives can be effectively converted to guaiacol derivatives, and guaiacol derivatives can be

518   converted to simple phenols. On long duration exposure to UV radiation, simple phenolics and

519   guaiacols can be converted to ring opened fragments such as C4-C6 linear carboxylic acids.[15,45]

520   These are finally mineralized to CO_2 and H_2O.

521   While wet ball milling of lignin-TiO_2 mixtures followed by photocatalysis is

522   demonstrated to be a promising method for the production of phenolics, the saturation of

523   catalytic activity after 6 h of UV exposure presents a reasonable challenge to adopt this method

524   for the treatment of lignin in a practical setting. One way to recover the catalyst is to first

525   separate the solid phase lignin-TiO_2 mixture after photocatalysis, and then dissolve it in alkaline

526   medium. This will solubilize lignin and adsorbed intermediates, and will free the active sites.

527   Thus, the degradation of lignin-TiO_2 suspension can be an initial step for alkaline degradation of

528   lignin. Importantly, this technique can be used to initially reduce the concentration of lignin,

529   especially from paper and pulp industry reject, to a reasonable value before subjecting it to other

530   processing techniques.

531   **4. Conclusions**

532   In this work, we have shown that wet milling of lignin and TiO_2 using polar solvents

533   improves the contact between lignin and TiO_2, thus facilitating lignin depolymerization to

534   produce valuable phenolic and aromatic compounds. For the first time, photocatalysis of lignin is

535   carried out by suspending the lignin-TiO_2 mixtures in water, without completely dissolving

536   lignin in alkaline medium. The change in intensity of emission lines in photoluminescence

537   spectra, appearance of carbon peak in XRD pattern and high onset degradation temperature in

538   TGA for WMW and WMA indicate that interactions may be involved when lignin and TiO_2 are

539   wet milled in presence of polar solvents. Wet milling in presence of water is shown to

540   depolymerize lignin besides causing particle size reduction and change in particle size

RSC Advances Accepted Manuscript

541   distribution. The extent of depolymerization caused by wet milling was evident from the

542   formation of water soluble phenolic compounds during the dark stirring period prior to

543   photocatalysis. Based on the concentration of phenolics produced during the dark stirring period,

544   various ball milled lignin-TiO_2 mixtures can be ranked as follows: wet milled (water) > wet

545   milled (hexane) > dry milled > wet milled (acetone). Compared to the dry milled and physical

546   mixtures, photocatalysis of wet milled mixtures resulted in high production of phenolics.

547   Based on the total phenolics produced during photocatalysis, the mixtures can be ranked as

548   follows: wet milled (acetone) > wet milled (water) > wet milled (hexane) > dry milled > physical

549   mixture. The major organic compounds identified via MALDI-TOF/MS and GC/MS include

550   ethyl benzene, acetovanillone, acetosyringone, syringaldehyde, styrene, acetyl vanillin, vanillin,

551   2,6-dimethoxy benzoquinone and diisobutyl phthalate. Importantly, the production of the first

552   four compounds in the above list increased with UV irradiation time. Moreover, a significant

553   reduction in molecular weight of lignin was observed during photocatalysis of wet milled (water)

554   mixture. The promising results of this study demonstrate that value added phenolic compounds

555   can be extracted from lignin via photocatalysis. The key challenges are to improve (a) the yield

556   and selectivity of phenolics by enhancing the contact between lignin and TiO_2, and (b) life time

557   of the catalyst by avoiding deactivation. More detailed studies are required to unravel the

558   mechanism of photocatalytic production of these organic compounds from lignin extracted from

559   different biomass feedstocks.

560

561

562

563

569

570 **References**

571 1. C. Xu, R. A. D. Arancon, J. Labidi and R. Luque*, Chem. Soc. Rev.*, 2014, **43**, 7485–7500.

572 2. P. Varanasi, P. Singh, M. Auer, P. D. Adams, B. A. Simmons and S. Singh, *Biotechnol.*

573   *Biofuels*, 2013, **6**, 1–9.

574 3. J. Zakzeski, P.C.A. Bruijnincx, A.L. Jongerius and B.M. Weckhuysen, *Chem. Rev.*, 2010,

575   **110**, 3552–3599.

576 4. J.H. Lora and W.G. Glasser, *J. Polym. Environ.*, 2002, **10**, 39–48.

577 5. M.P. Pandey and C.S. Kim, *Chem. Eng. Technol.*, 2011, **34**, 29–41.

578 6. H. Lange, S. Decina and C. Crestini, *Eur. Polym. J.,* 2013, **49**, 1151–1173.

579 7. G. Chatel and R.D. Rogers, *ACS Sustainable Chem. Eng.*, 2014, **2**, 322–339.

580 8. O.A. Makhotkina, S.V. Preis and E.V. Parkhomchuk, *Appl. Catal. B*, 2008, **84**, 821–826.

581 9. R. Prado, X. Erdocia and J. Labidi, *Chemosphere*, 2013, **91**, 1355–1361.

582 10. M. Zhang, F. L.P. Resende and A. Moutsoglou, *Fuel*, 2014, **116**, 358–369.

583 11. W.Y. Teoh, J.A. Scott and R. Amal, *J. Phys. Chem. Lett.,* 2012, **3**, 629−639.

584 12. R. Vinu and G. Madras, Photocatalytic degradation of water pollutants using nano-TiO_2, in

585   *Energy efficiency and renewable energy through nanotechnology*, Ed. L. Zang, Springer-

586   Verlag, London, 2011*,* 625–677.

587 13. U. I. Gaya and A. H. Abdullah, *J. Photochem, Photobiol. C: Photochem. Rev.,* 2008, **9**, 1–12.

588 14. C. Heitner, D.R. Dimmel and J.A. Schmidt, *Lignins and Lignans: Advances in Chemistry*,

589   CRC press, Boca Raton, FL, 2010.

590 15. C.M. Felício, A.E.H. Machado, A. Castellan, A. Nourmamode, D.S. Perez and R. Ruggiero,

591   *J. Photochem. Photobiol. A: Chem.,* 2003, **156**, 253–265.

592   16. K. Kobayakawa, Y. Sato, S. Nakamura and A. Fujishima, *Bull. Chem. Soc. Jpn.*, 1989, **62**,
593   3433–3436.

594   17. K. Tanaka, R.C.R. Calanag and T. Hisanaga, *J. Mol. Catal A: Chem.*, 1999, **138**, 287–294.

595   18. A.E.H. Machado, A.M. Furuyama, S.Z. Falone, R. Ruggiero, D.D.S. Perez and A. Castellan,
596   *Chemosphere*, 2000, **40**, 115–124.

597   19. M. Ksibi, S.B. Amor, S. Cherif, E. Elaloui, A. Houas and M. Elaloui, *J. Photochem.*
598   *Photobiol. A: Chem.*, 2003, **154**, 211–218.

599   20. S.K. Kansal, M. Singh and D. Sud, *J. Hazard. Mater.*, 2008,**141**, 581–590.

600   21. Y.S. Ma, C.N. Chang, Y.P. Chiang, H.F. Sung and A.C. Chao, *Chemosphere*, 2008, **71**, 998–
601   1004.

602   22. K. Kamwilaisak and P.C. Wright, *Energy Fuels*, 2012, **26**, 2400−2406.

603   23. H. Li, Z. Lei, C. Liu, Z. Zhang and B. Lu, *Bioresour. Technol.*, 2015, **175**, 494–501.

604   24. G. Brodeur, E. Yau, K. Badal, J. Collier, K.B. Ramachandran and S. Ramakrishnan, *Enzyme*
605   *Res.,* 2011, **2011**, 1–17.

606   25. Y. Yamashita, C. Sasaki and Y. Nakamura, *Carbohydr. Polym.,* 2010, **79**, 250–254.

607   26. Z.X. Lin, H. Huang, H.M. Zhang, L. Zhang, S. Yan and J.W. Chen, *Appl. Biochem.*
608   *Biotechnol.*, 2010, **162**, 1872–1880.

609   27. H. J. Kim, S. Lee, J. Kim, R. J. Mitchell and J. H. Lee, *Bioresour. Technol.*, 2013, **144**, 50–
610   56.

611   28. D.J. Nowakowski, A.V. Bridgwater, D.C. Elliott, D. Meier and P. de Wild, *J. Anal. Appl.*
612   *Pyrol.*, 2010, **88**, 53–72.

613   29. K.L. Willett and R.A. Hites, *J. Chem. Ed.*, 2000, **77**, 900–902.

614   30. R. Vinu and G. Madras, *J. Indian Inst. Sci.*, 2010, **90**, 189–230.

615   31. Y. Qu, H. Luo, H. Li and J. Xu, *Biotech. Rep.,* 2015, **6**, 1–7.

616   32. V. K. Ahluwalia, *Text Book of Organic Chemistry,* ANE Books, 2015.

617   33. M. A. Henderson, *Langmuir*, 2005, **21**, 3443–3450.

618   34. S. Rudatin, Y.L. Sen and D.L. Woerner, Association of kraft lignin in aqueous solution, in
619   Lignin, Chapter 11, *ACS Symposium Series*, 1989, **379**, 144–154.

620   35. W. Qin, Z.-M. Zheng, P. Kang, C. Dong and Y. Yang, *Bioresources*, 2014, **9**, 628–641.

621   36. J. Kim, B.S. Kwak, and M. Kang, *Bull. Korean Chem. Soc.*, 2010, **31**, 344–350.

622   37. V. Nair, A. Panigrahy and R. Vinu, *Chem. Eng. J.*, 2014, **254**, 491–502

623 38. C.G. Boeriu, D. Bravo, R.J.A. Gosselink and J.E.G. van Dam, *Ind. Crop. Prod.*, 2004, **20**,
624   205−218.

625 39. R. Parthasarathi, V. Subramanian and N. Sathyamurthy, *J. Phys. Chem. A*, 2005, **109**, 843–
626   850.

627 40. K. Nagaveni, M.S. Hegde and G. Madras, *J. Phys. Chem. B*, 2004, **108**, 20204–20212.

628 41. L. Cai, Q. Long and C. Yin, *Appl. Surf. Sci.*, 2014, **319**, 60–67.

629 42. I. Chung, B. Lee, J. He, R.P.H. Chang and M.G. Kanatzidis, *Nature*, 2010, **485**, 486–489.

630 43. S.-H. Li, S. Liu, J.C. Colmenares and Y.-J. Xu, *Green Chem.,* 2015, doi:
631   10.1039/c5gc02109j.

632 44. A. Toledano, L. Serrano, A. Pineda, A.A. Romero, R. Luque and J. Labidi, *Appl. Catal. B:*
633   *Environ.*, 2014, **145**, 43–55.

634 45. R. Vinu, S. Polisetti and G. Madras, *Chem. Eng. J.*, 2010, **165**, 784–797.

635

636

637

638

639

640

641

642

643

644

645

646

647

648

649

650 **List of Tables**

660 **List of Figures**

678   acetovanillone, 3 –2,6-dimethoxybenzoquinone, 4 – syringaldehyde, 5 – diisobutyl phthalate, 6 –

679   styrene, 7- vanillin, 8 – acetyl vanillin, 9 – acetosyringone.

680   **Figure 11.** Variation of concentration (in mg g_{lignin}^{-1}) of the major products obtained in the DCM

681   extract from photocatalysis of WMW lignin-TiO_2 mixture.

682

683

684

685

686

687

688

689

690

691

692

693

694

695

696

697

698

699

700

701

702   Table 1. List of the existing studies on photocatalytic degradation of lignin reported in the
703   literature.

Sl. No.	Type of lignin	Photocatalyst	Reaction conditions	Products	Reference
1	Kraft lignin	TiO_2	25 g L^{-1} rutile TiO_2 in 0.02 wt % of lignin in 20 mL of solution ; 500 W HPML; pH > 8	Methanol, ethanol, formaldehyde, formic acid, oxalic acid and traces of methane and ethane	Kobayakawa et al. (189)[16]
2	Coniferous wood lignin	TiO_2	0.7 g L^{-1} catalyst ; 0.01 % of lignin in 300 mL reaction solution; 100 W HPML	Carboxylate, aldehyde	Tanaka et al. (1999)[17]
3	Peroxy formic acid lignin	TiO_2	5 mg L^{-1} catalyst ; Lignin dissolved in 1:4 v/v ethanol-water mixture at 250 mg L^{-1} in 25 ml of reactant solution; 400 W MPML	Complete mineralization	Machado et al. (2000)[18]
4	Lignin precipitate from black liquor	TiO_2	1 g L^{-1} catalyst; 330 mg L^{-1} lignin in 1 L of solution; 9 pH ; 125 W HPML	Vanillin, coniferylic alchol, vanillic acid, p-coumanic acid, syringaldehyde	Ksibi et al. (2003)[19]
5	Wheat straw lignin	TiO_2-ZnO	1 g L^{-1} catalyst; 11 pH; 30W UV tubes	Complete mineralization	Kansal et al. (2008)[20]
6	Synthetic lignin	Pt-TiO_2	1 g L^{-1} catalyst ; 251 mg L^{-1} of reactant mixture; 11 pH; 35W UV tubes	Mineralization monitored using dissolved organic carbon content	Ma et al. (2008)[21]
7	Kraft lignin	TiO_2- laccase	3 g L^{-1} of photocatalyst; 5.55 g L^{-1} H_2O_2 ; laccase in 1 g L^{-1} lignin in 10 mL of reactor	Succinic acid, malonic acid, acetic acid, vanillin	Kamwilaisak and Wright (2012)[22]

			solution; 5 pH ; 24W UV tubes		
8	Organosolv lignin black liquor	TiO_2	2 g L^{-1} catalyst; was added to 50 mL of lignin; 300W UV lamp	Syringol, pyrocatechol, vanillin, syringaldehde, sinapyladehyde	Prado et al. (2013)[9]
9	Alkali lignin	Ag-AgCl-ZnO	0.5 g L^{-1} catalyst ; 50 mg L^{-1} Lignin solution; 11 pH ; solar light	Methane	Li et al. (2015)[23]
10	Industrial lignin	Aeroxide TiO_2	0.4 g of 1:1 w/w Lignin-TiO_2 ball milled mixtures suspended in 200 mL aq. medium; natural pH; 125 W HPML	Ethyl benzene, vanillin, acetovanillone, acetosyrigone, syringaldehyde	This work

704   HPML - High Pressure Mercury Lamp, MPML - Medium Pressure Mercury Lamp

705

706

707

708

709

710

711

712

713

714

715

716

717

32

718   Table 2. Maximum concentration of phenolics produced in the aqueous phase via both dark

719   mixing and photocatalysis, and % contribution by photocatalysis for physical and ball milled

720   mixtures of lignin with TiO_2.

	C_{max} (mg L^{-1})	% Contribution by photocatalysis
Untreated lignin	88	0
Physical mixture of untreated lignin with TiO_2	94	6
Physical mixtures		
Dry milled lignin and TiO_2	127	38
Wet milled (acetone) lignin and TiO_2	77	58
Wet milled (hexane) lignin and TiO_2	116	24
Wet milled (water) lignin and TiO_2	183	13
Ball milled mixtures		
DM	155	20
WMA	143	55
WMH	215	38
WMW	464	42

721

722

723

724

725

726

727

728

729

730

731

732

733   Table 3. Variation of weight average and number average molecular weights of wet milled

734   (water) mixture (WMW) of lignin and TiO_2 during dark stirring and UV irradiation period.

735

	Time (min)	M_w (g mol^{-1})	M_n (g mol^{-1})
Before wet milling		1980	450
Dark stirring period	-180$^{\#}$	1777	400
	-120	1722	300
UV irradiation period	0	1590	485
	60	1418	250
	180	1160	265
	360	1040	260

736

737   * It is important to note that the above molecular weight values are based on PMMA standards, and cannot be
738   compared with the reported molecular weight of lignin, which is 2500-3400 g mol^{-1}. $^{\#}$Corresponds to lignin+TiO_2
739   after wet milling in water medium.

740

741

742

743

744

745

746
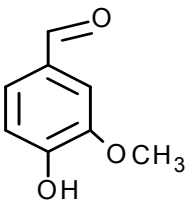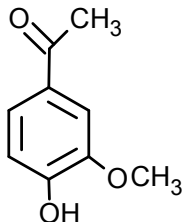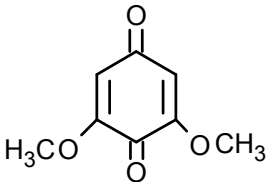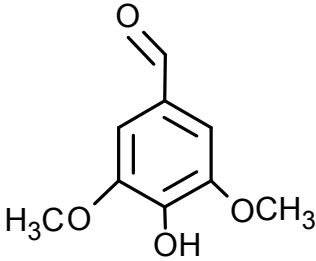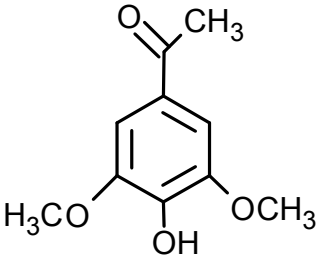
747
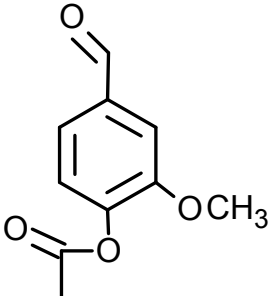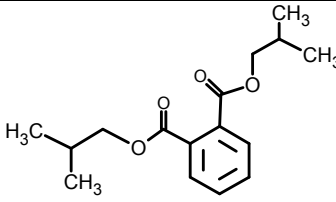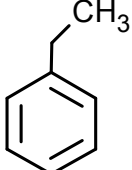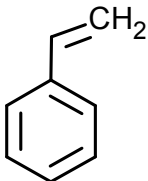
748

749

750

751   Table 4. Major products obtained from photocatalysis of WMW lignin-TiO$_2$ mixture identified

752   by GC/MS.

Compounds identified in the DCM extract via GC/MS	Molecular weight (g mol $^{-1}$)	Structure	% Similarity with NIST	Major ions
Vanillin	152.15		95	51, 53, 65, 81, 93, 109, 123, 137, 151
Acetovanillone	166.17		90	43, 52, 65, 73, 80, 93, 95, 108, 123, 136, 151, 166
2,6-Dimethoxy benzoquinone	168.15		85	53, 59, 69, 80, 82, 97, 109, 112, 123, 127, 138, 169, 170
Syringaldehyde	182.17		93	51, 65, 79, 93, 96, 111, 139, 153, 167, 182, 183
Acetosyringone	196.19		95	43, 65, 67, 79, 85, 93, 108, 123, 138, 153, 167, 181, 196

35

Acetyl vanillin	194.18		90	44, 52, 65, 79, 122, 152
Diisobutyl phthalate	278.35		91	41, 57, 65, 76, 104, 121, 149, 150, 167, 223
Ethyl benzene	106.17		98	51, 65, 74, 77, 91, 106, 107
Styrene	104.15		95	43, 50, 51, 77, 78, 84, 104

753

754

755

756

757

758

759

760

761
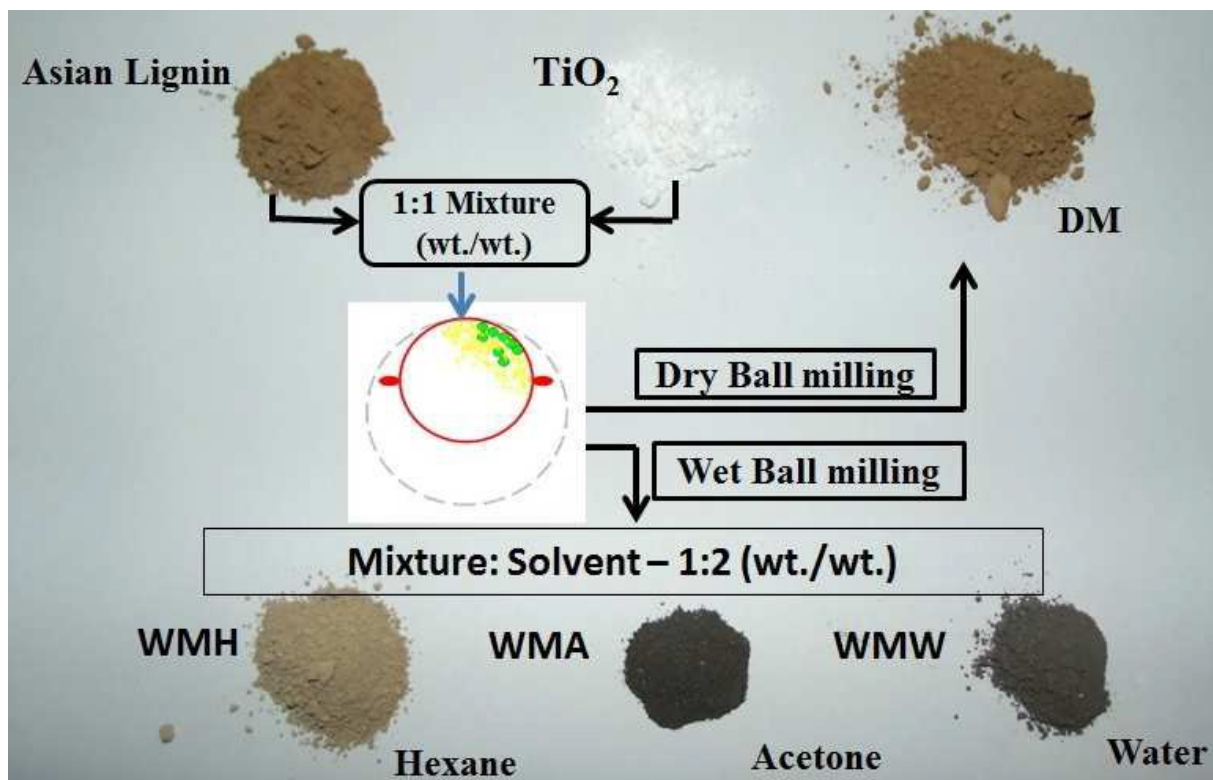
Figure 1. Preparation methodology of various ball milled lignin-TiO$_2$ mixtures.
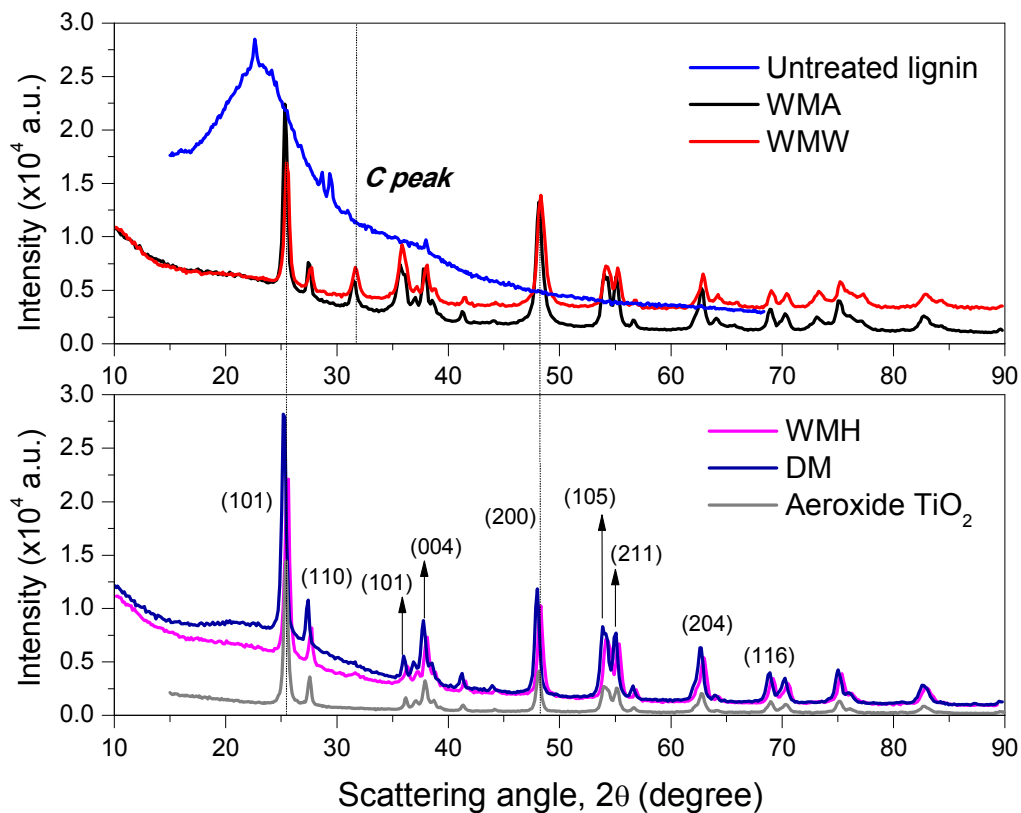
765

766   Figure 2. XRD patterns of TiO_2, lignin and different wet milled mixtures of the two.

767

768
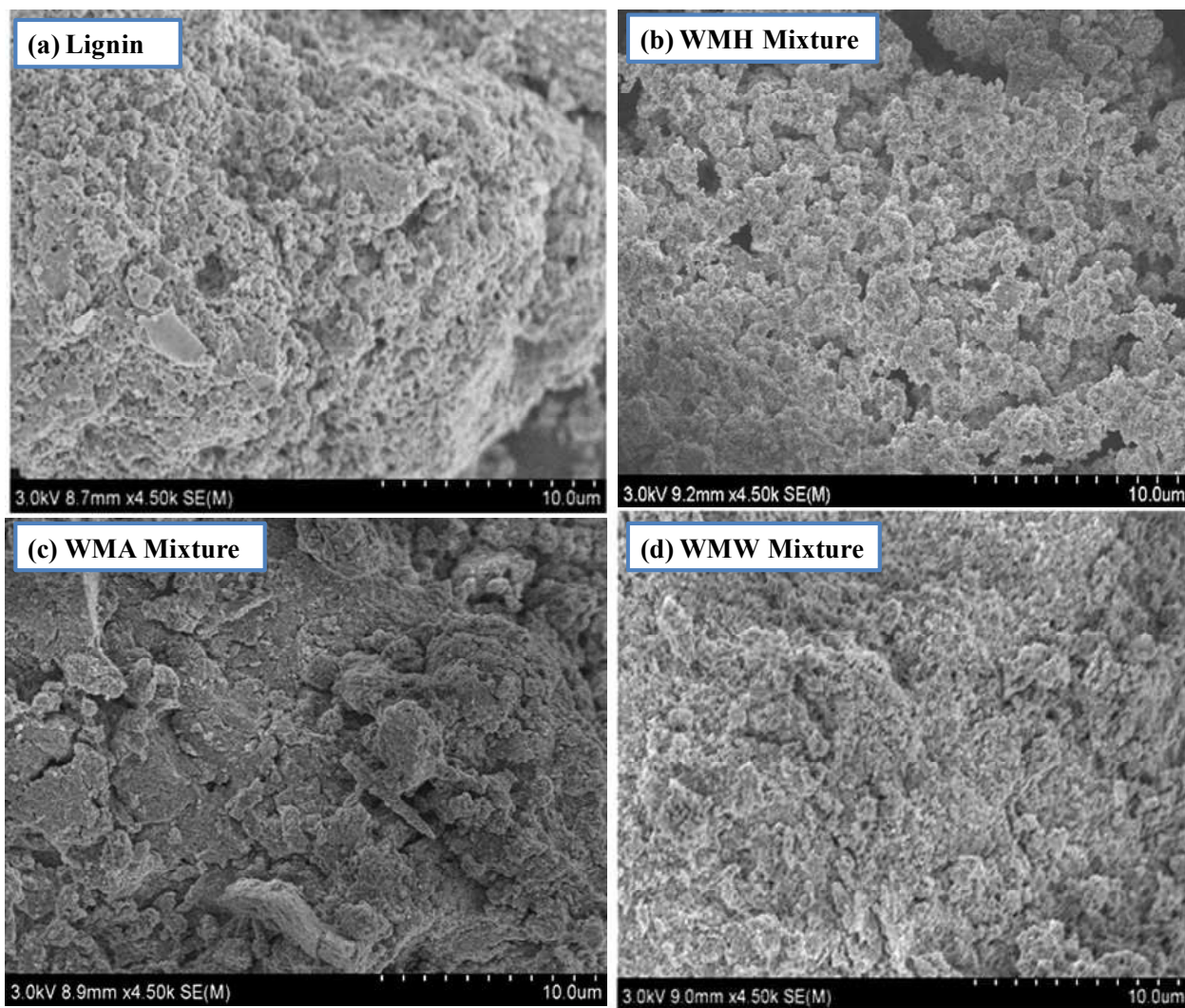
769

770

771　　Figure 3. SEM images of (a) Lignin (b) WMH (c) WMA, and (d) WMW lignin-TiO_2 mixtures.

772

773

774

775

776

777

778

779
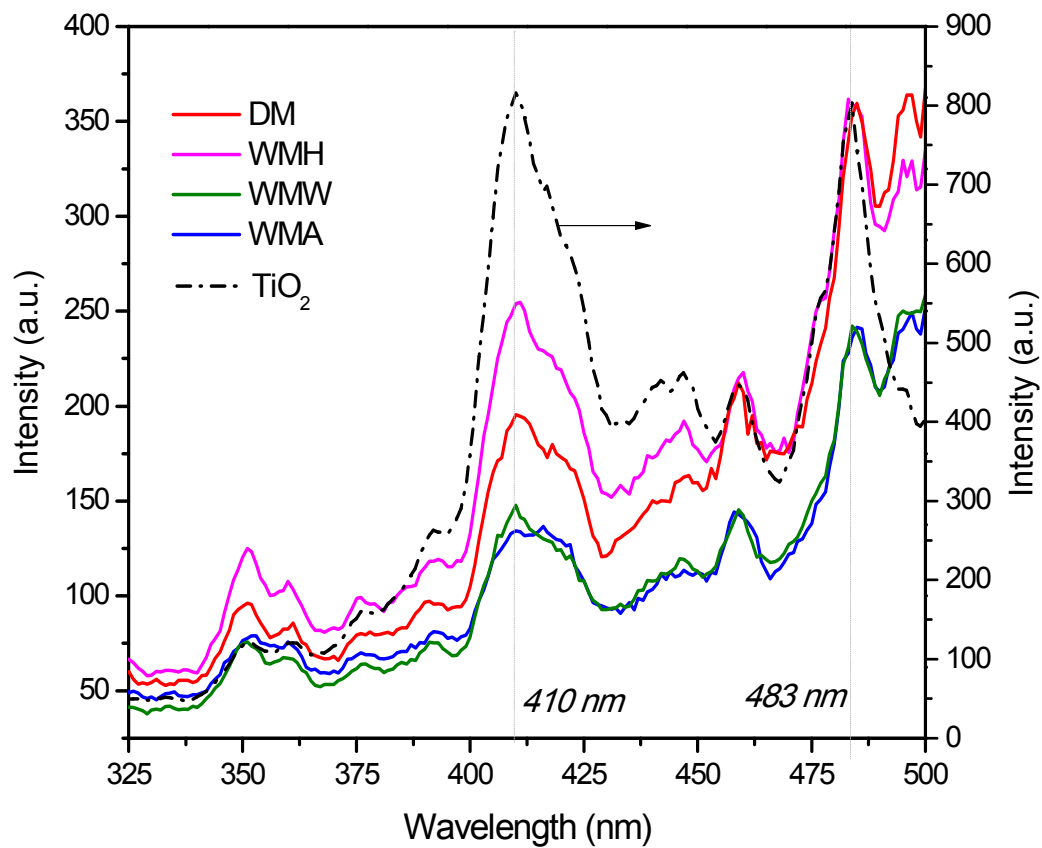
Figure 4. Photoluminescence spectra of TiO_2 and wet ball milled mixtures of lignin and TiO_2.
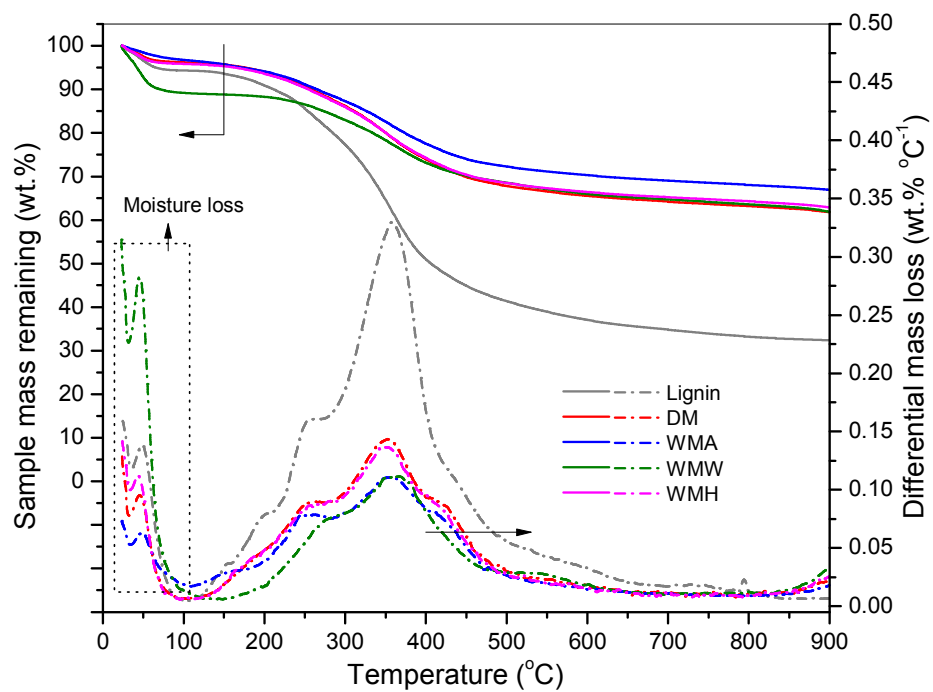
Figure 5. Mass loss and differential mass loss profiles of lignin and various lignin-TiO_2 mixtures.
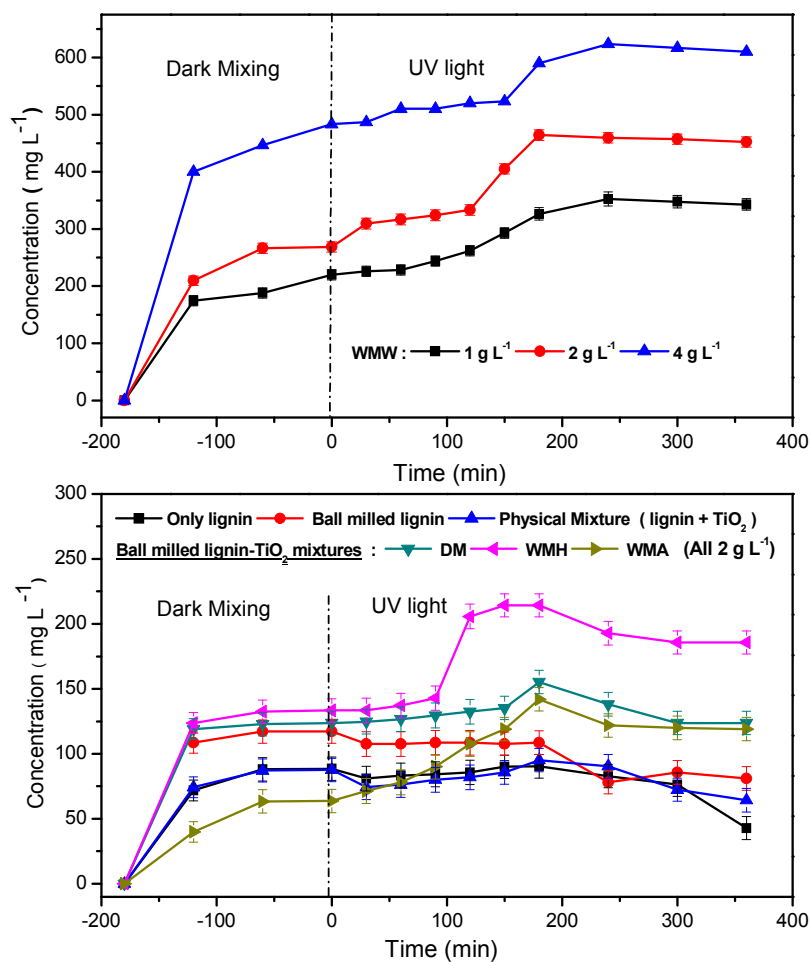
792

793   Figure 6. Concentration profiles of phenolic compounds formed during dark mixing and

794 photocatalysis of various lignin-TiO_2 mixtures of 2 g L^{-1} concentration in aqueous medium.
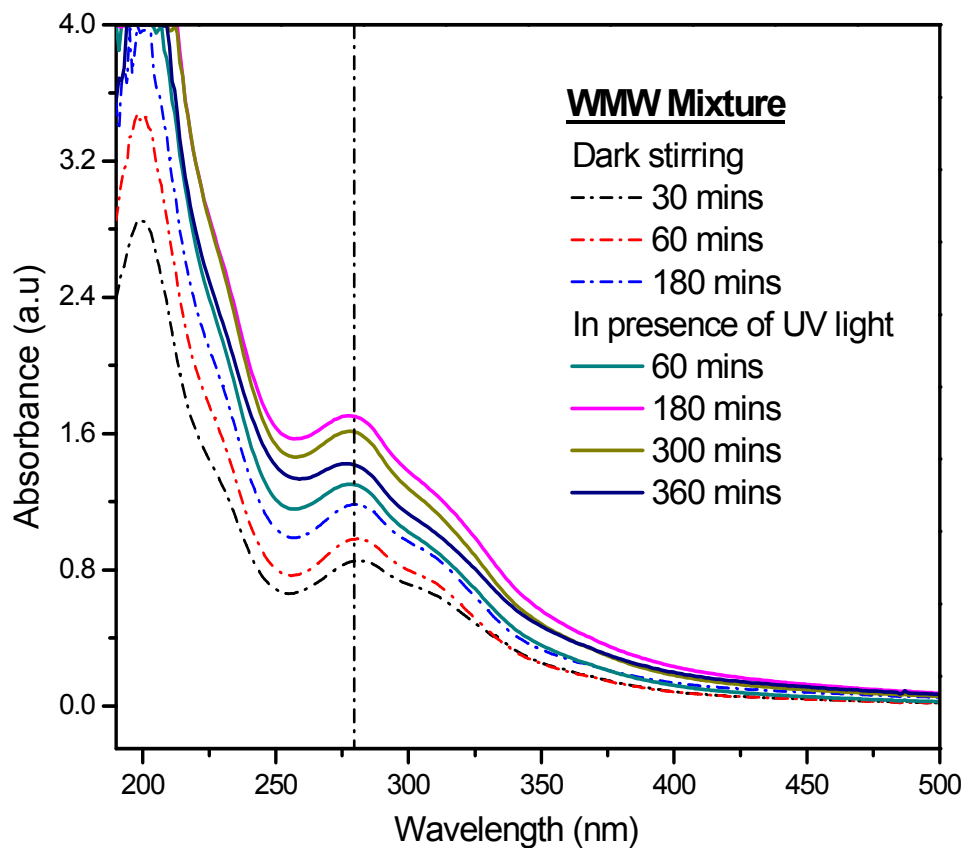
795

796

797

798

799

800

801
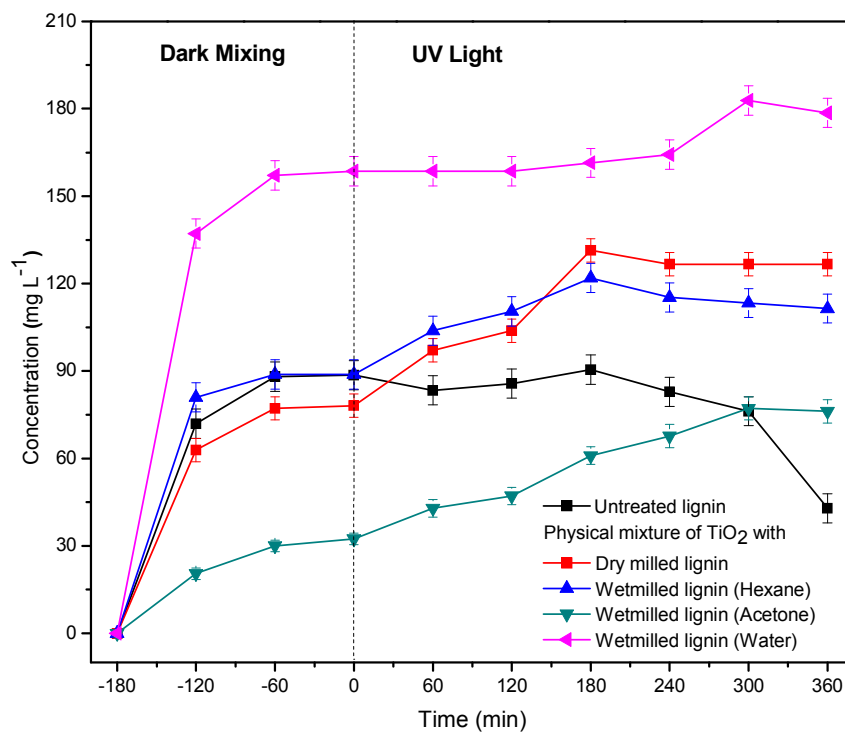
802

803   Figure 7. Production of phenolics during dark mixing and UV irradiation from 2 g L^{-1} of physical

804   mixtures of lignin and TiO$_2$. Importantly, TiO$_2$ was not mixed with lignin during ball milling, but

805   added only during the photocatalysis experiments.

Figure 8. UV-visible spectra depicting the evolution of phenolics during dark stirirng and photocatalysis of WMW lignin-TiO$_2$ mixture (2 g L^{-1}).
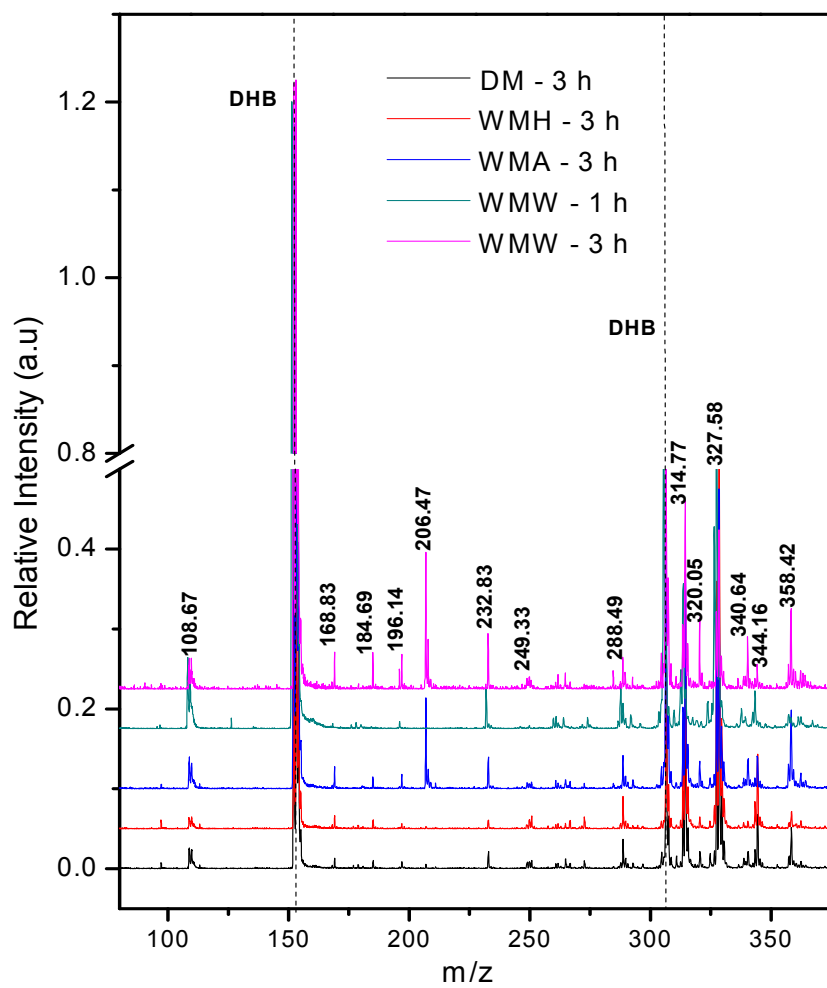
817

818   Figure 9. MALDI – TOF mass spectra of the liquid phase after subjecting various ball milled

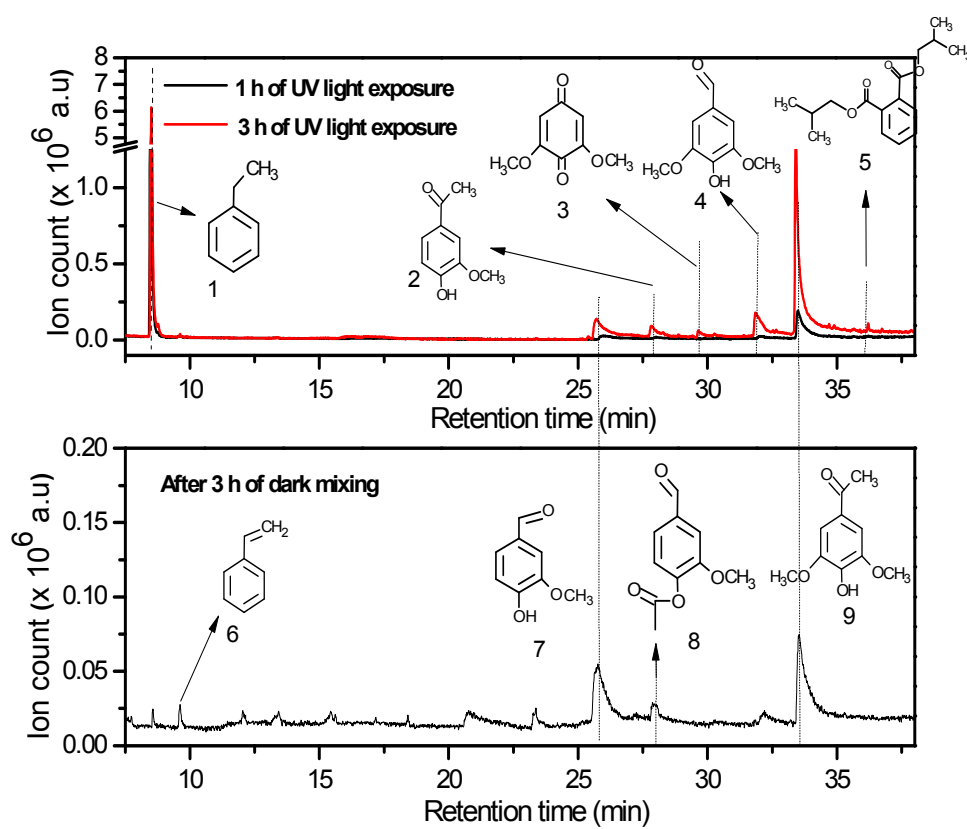819   mixtures to UV irradiation for different time periods.
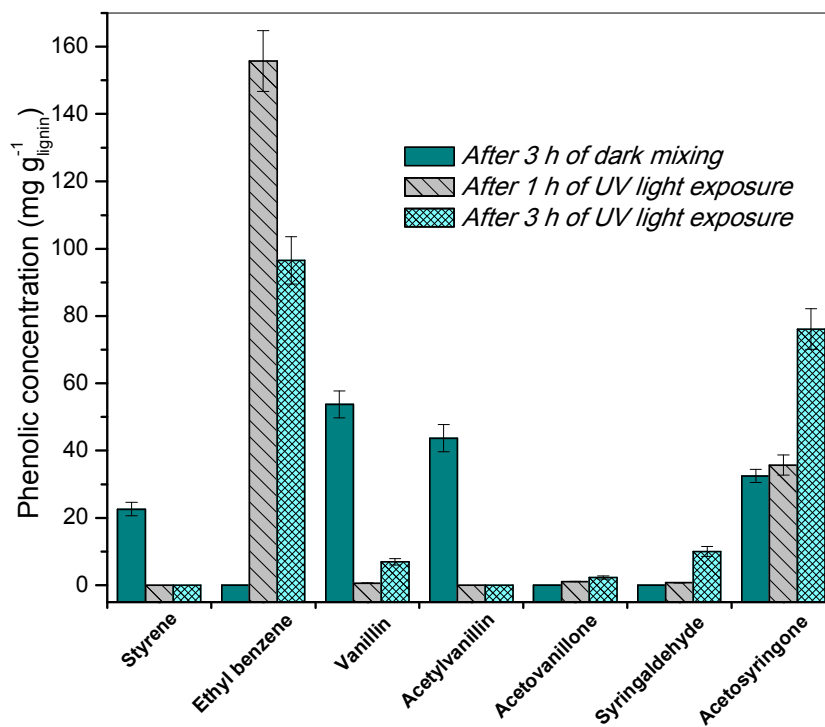
820

821

822

823

824

825

Figure 10. GC/MS total ion chromatograms of DCM extract obtained from photocatalysis of WMW liginin-TiO$_2$ mixture at different durations. The peaks correspond to 1– ethyl benzene, 2– acetovanillone, 3 –2,6-dimethoxybenzoquinone, 4 – syringaldehyde, 5 – diisobutyl phthalate, 6 – styrene, 7- vanillin, 8 – acetyl vanillin, 9 – acetosyringone.

830

831   Figure 11. Variation of concentration (in mg g_{lignin}^{-1}) of the major products obtained in the DCM

832   extract from photocatalysis of WMW lignin-TiO_2 mixture.
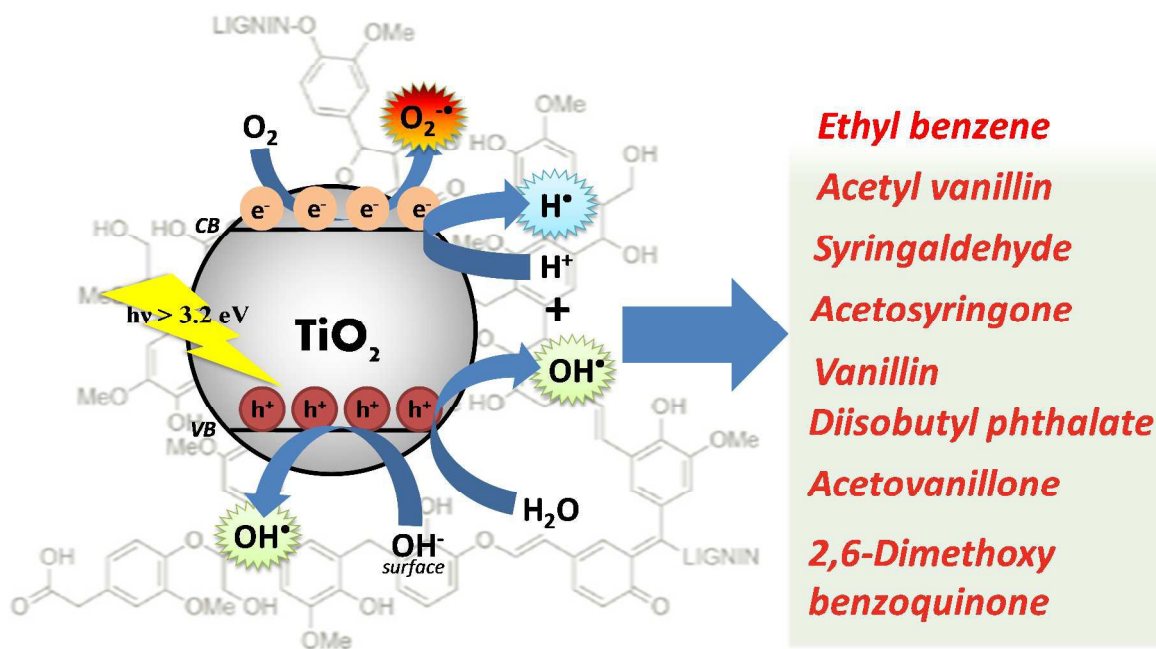
833

Production of Phenolics via Photocatalysis of Ball Milled Lignin-TiO$_2$ Mixtures in Aqueous Suspension

Vaishakh Nair,[a] Piyali Dhar,[a] R.Vinu[a,b,*]

[a] Department of Chemical Engineering, Indian Institute of Technology Madras, Chennai – 600036, India

[b] National Center for Combustion Research and Development, Indian Institute of Technology Madras, Chennai – 600036, India

Graphical and Textual Abstract

Ethyl benzene
Acetyl vanillin
Syringaldehyde
Acetosyringone
Vanillin
Diisobutyl phthalate
Acetovanillone
2,6-Dimethoxy benzoquinone

This work demonstrates the production of value added phenolics and aromatics via UV photocatalysis of lignin-TiO$_2$ mixtures prepared by wet ball milling using different solvents.

* Corresponding Author. Phone: +91-44-2257 4187. E-mail: vinu@iitm.ac.in (R. Vinu)